Appl. Phys. A 76, 957–959 (2003)
DOI: 10.1007/s00339-002-1757-1

Applied Physics A
Materials Science & Processing

M. SENDOVA✉
K. WILLIS

Spiral and curved periodic crack patterns in sol-gel films

Division of Natural Sciences, New College of Florida, Sarasota, FL 34238, USA

Received: 25 March 2002/Accepted: 1 July 2002
Published online: 17 December 2002 • **© Springer-Verlag 2002**

ABSTRACT Thin silicate sol-gel films with four different crack patterns were created reproducibly by controlling the film deposition parameters. The crack geometry, periodicity, and amplitude were studied experimentally as a function of the film thickness, curing time, and temperature. Direct evidence was found that the physical interplay between stress relief through film cracking and stress relief through film warping results in sawtooth, spiral, closed loop, or straight line crack trajectories.

PACS 61.43.Er; 62.20.Mk; 68.35.Gy; 68.37.-d

1 Introduction

Fascinating crack patterns and the puzzle of their origin have long occupied the thoughts of scientists from various fields. The problem of crack pattern formation has theoretical [1–4] as well as practical significance in mechanics, physics and the chemistry of materials [5–12], and can be a subject of study in the physics of self-organizing phenomena as well. Here, we discuss our experiments with silicate sol-gel films as they relate to crack patterns. In a controlled and reproducible manner we were able to create four distinct types of crack patterns: straight-line cracks, curved closed-loop cracks (Fig. 1), crescent (sawtooth) periodic cracks (Fig. 2) and spiral cracks (Fig. 3). Through these experiments, we have found a relationship between the geometrical parameters of the cracks and some of the properties of the films. We suggest a phenomenological explanation based on film warping due to stress non-uniformity created in the drying stage of the sol-gel materials [13].

2 Experimental

To begin the experiments, the films were deposited on glass and polished metal substrates by spin-coating of silicate sol (Filmtronics Inc) using a spin coater manufactured by Specialty Coatings Systems Inc. The film thickness was controlled by the rotational speed of the spin-coater. The structures

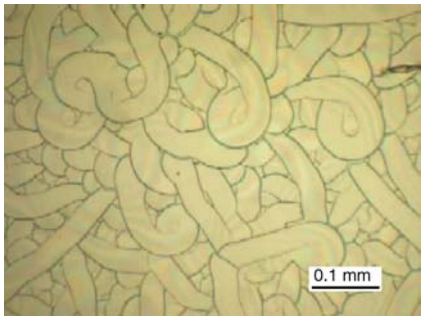

FIGURE 1 Curved, closed-loop crack pattern in 1.2 μm film on glass

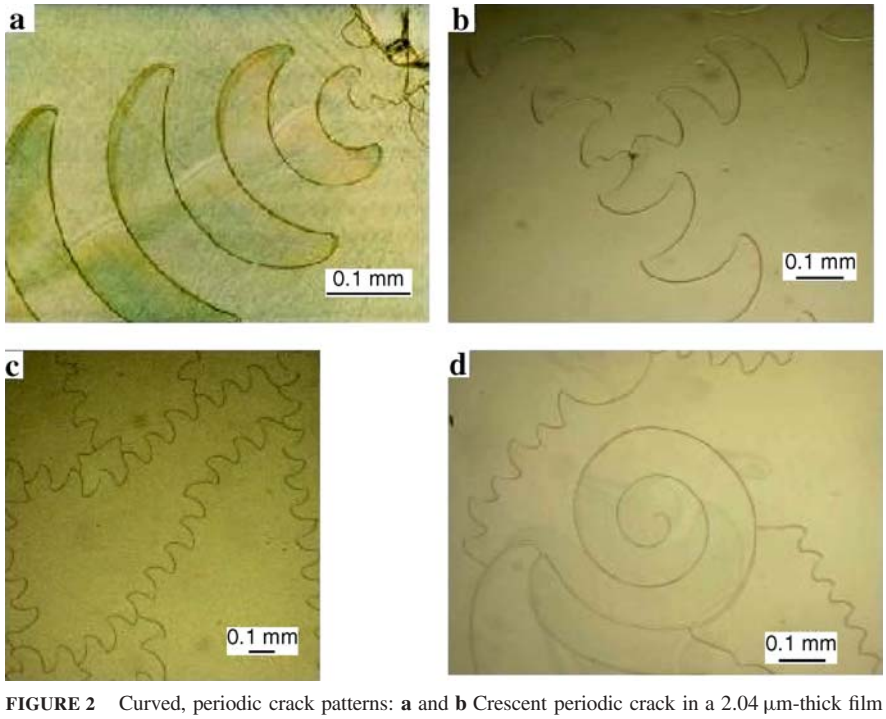

FIGURE 2 Curved, periodic crack patterns: **a** and **b** Crescent periodic crack in a 2.04 μm-thick film on polished metal. **c** A network of periodic cracks in a 2.04 μm-thick film on glass. **d** Coexistence of spiral and periodic cracks in a 2.04 μm-thick film on glass

✉ Fax: +1-941-359-4396, Email: sendova@ncf.edu

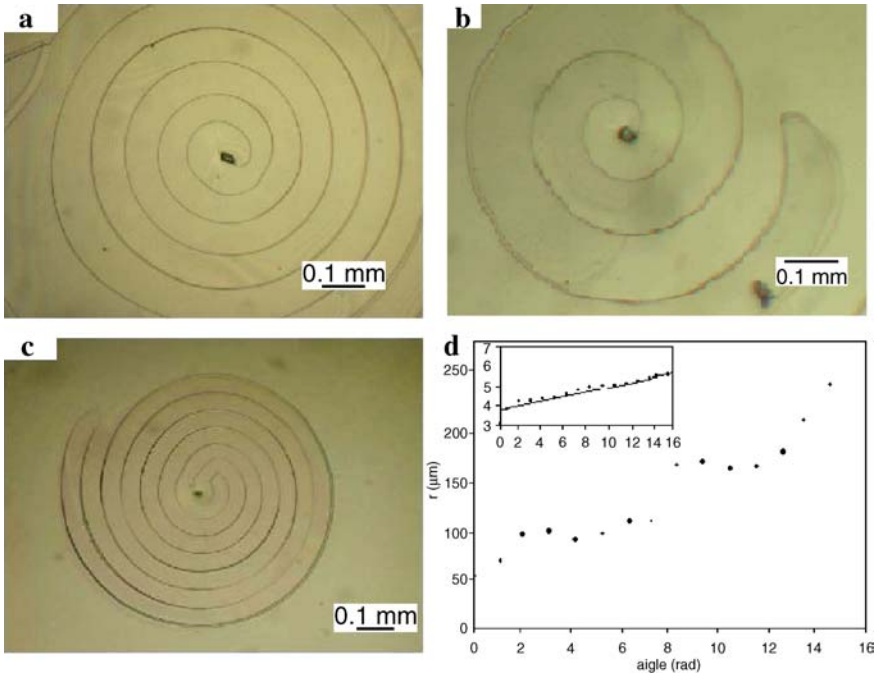

FIGURE 3 Spiral cracks in a 2.04 μm-thick film on glass: **a** and **b** A single-arm spiral. **c** A double-arm spiral. **d** Graph of the spiral radius vs the polar angle for the spiral crack shown in **b**. In the *inset* of this graph, the same data with a linear fit of the logarithm of the radius vs the polar angle are shown

studied were composed of two layers, deposited and dried in two consecutive steps. The combined thickness of the layers was not greater than 2 μm. In these experiments, the deposition parameters of the second layer were kept constant.

Sol-gel films are very suitable for promoting spiral and curved periodic cracks because of their distinct physical properties, related to the high degree of shrinkage of the gel network during the drying stage [13]. This allows conditions to be set for creating differences in the shrinkage rate from surface to center even in relatively thin films. In our experiments, depositing a second layer after the drying stage of the first layer causes high non-uniformity in the contraction of the film as a whole. The spin speed, the temperature of drying and the time duration of drying of the first layer were varied in a systematic manner. The cracks in the films were studied by optical microscope, and the images were digitally recorded and analyzed.

3 Results and discussion

On a single slide, we observed crescent periodic crack patterns (Fig. 2), differing in amplitude and wavelength (period). All types of cracks discussed here were through the whole film and reached the substrate. This was confirmed by imaging the crack with an atomic force microscope and measuring its depth. The amplitude was the span of the crack perpendicular to the general direction of the crack propagation. The amplitude of the cracks could be as low as 10 μm, and as high as 800 μm. The period of the sawtooth pattern also varied over a wide range. The crack pattern wavelengths could be as low as 35 μm and as high as 840 μm. Empirically, there was a linear proportionality between the amplitude of the crack pattern and its period for films of the same thickness. The slope of the best linear fit to the amplitude vs period data points depended on the thickness of the film – the thicker the film was, the smaller was the slope. When comparing the minimum observable period (the "wavelength threshold") of the crack patterns to the film thickness, it was obvious that the thicker the film was, the higher was the wavelength threshold. When comparing samples with the first layer deposited at the same spin speed and dried at the same temperature, but with increasing drying time, there was a tendency of decreasing wavelength threshold. This tendency was more pronounced in thicker films (deposited at smaller spin speeds) than in thinner ones. When increasing the drying temperatures, there was a decrease in the wavelength threshold with temperature in samples deposited at the same spin speed and dried for the same drying time.

Spiral cracks (Fig. 3) were observed on the same samples where the periodic, crescent-type cracks occurred (Fig. 2d). This is the first reporting of a double-arm spiral crack (Fig. 3c). Usually the crack started from a defect in the film, such as an inclusion or a high stress point, and continued outward along a spiral trajectory. In the experiments of Neda et al. [4], film delamination proceeded from the outside in, resulting in spirals that propagate inward. The conical spiral crack that formed during the shrinkage of a silica-based sol-gel sheet of material has been described by Hull [9]. These cracks had diameters similar to the cracks we observed; about 1 mm. However, they were developed due to the internal stress in a much thicker specimen compared with our 2 μm films, and they started from the periphery and created a spiral propagating inward. In contrast, our cracks always propagated from the center outward. The speed of the tip of the crack varied. The tips tended to slow down as

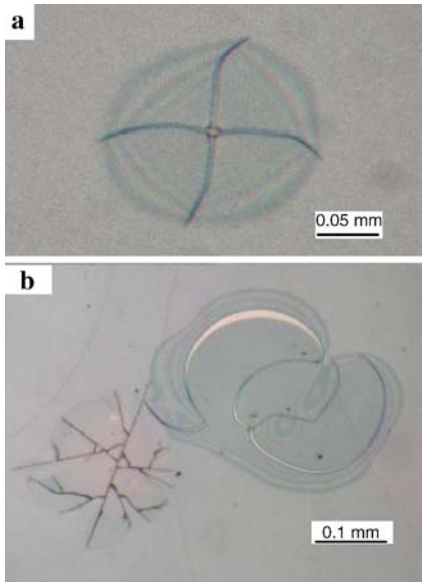

FIGURE 4 Interference patterns showing warping of the film. The film thickness is 2.04 μm, the substrate is glass and there is a 10 nm gold film between the film and the substrate to increase the interference contrast. **a** Straight cracks propagate as long as there is no warping of the film. **b** Coexistence between curved and straight cracks

the radius of the spiral increased, or they propagated in jumps covering 180° after considerably decreasing their speed.

The spirals could be interpreted as being either linear or logarithmic. The equation of an equiangular (or logarithmic) spiral in polar coordinates is $r(\theta) = r_o e^{k\theta}$, where r is the distance from the origin, θ is the angle from the x-axis, and r_o and k are constants. The dimensionless constant k characterizes the tightness of the spiral, and it is related to the angle between the tangent and the radial line at a point of the spiral, $\psi = \cot^{-1} k$. The spiral radius r, as a function of the polar angle, θ, for the spiral shown in Fig. 3b, is plotted in Fig. 3d. In the inset, the linear fit of the logarithm of the radius versus the polar angle is shown. The slope of the line through the points gives the constant k of a given spiral, which in our experiment was between 0.08 and 0.18 for various spirals. Our experiments showed a tendency for k to decrease with film thickness, contrary to Neda et al. [4], who observed spiral cracks with constant k between 0.06 and 0.08, and independent of the layer thickness. Since the power of the exponent was relatively small, it was possible for the data to be fitted with a linear function as well. We analyzed the data from 20 spirals, and we found that the quality of the linear and the exponential fits on average differed by not more than 2% both ways.

All experimental data and observations can be explained if curved crack formation due to local warping of the film is assumed. As long as the film stays flat and attached to the surface, the cracks propagate along straight lines, as seen in Fig. 4b. A crack can start from a defect and can propagate along a straight line, but further on, the crack can promote detachment followed by buckling of the film. The latter can promote curving of the crack itself. Such feedback stimulates the development of rather organized, periodic and symmetrical crack patterns. Interference fringes observed in the area of the crack tips as soon as they start to curve (Fig. 4a) confirm the suggested mechanism of crack formation. Interference fringes are due to the thin layer (not more than 1 μm of air between the film and the substrate. The density and the shape of the fringes are an indication of the curvature and the distance between the substrate and the detached film. Spiral cracks are a result of bowl-shaped curving of the film. Crescent periodic cracks (Fig. 2) might be due to cylindrical buckling (wrinkles) of the film. The general direction of propagation of such cracks is along the axis of the cylinder.

The difference in shrinkage rate between the two surfaces of the film was the cause of so-called drying stress. The drying stress was considerably larger than the stress in the film created by the difference in the thermal expansion coefficients of the film and the substrate. The fact that the same crack patterns were observed regardless of the type of the substrate on which the film was deposited is an experimental proof that the adhesion of the film and its thermal mismatch with the substrate are small effects in comparison to the effect of the drying stress. The shrinkage of the network determines properties of the film, such as porosity and permeability, which in turn determine the stress distribution in the film [13]. The asymmetry of the stress distribution forces the film to warp. The thickness of the film determines the maximum possible curvature (the smallest radius) when buckling occurs. In turn, the maximum curvature in the area of buckling determines the wavelength threshold of the periodic cracks and the constant of the spiral cracks. The linear proportionality between the amplitude and the wavelength of the periodic crescent cracks is another proof of the idea that buckling promotes these types of crack. The drying regime of the first layer controls to a great extent the non-uniformity of the film contraction, which in turn affects the curvature of warping. Increasing the drying time at a given temperature leads to larger warping curvatures. Increasing the drying temperature while maintaining the same drying time has a similar effect. Experimentally, the effect of the increased drying rate on the first layer is demonstrated by reducing the wavelength threshold in the periodic crescent cracks.

4 Summary

In a controlled and reproducible manner, we were able to create four distinctive types of crack patterns. Their geometric characteristics were related to the thickness of the film and the deposition parameters. There is evidence that the observed curved periodic crack patterns are a result of local warping of the film caused by the stress nonuniformity created at the drying stage of the sol-gel material.

ACKNOWLEDGEMENTS We thank Prof. M. Bradley, Prof. G. Ruppeiner and M. Taylor for discussions and suggestions. This work was supported by the Research and Creative Scholarship Grant Program of the University of South Florida.

REFERENCES

1 Z.C. Xia, J.W. Hutchinson: J. Mech. Phys. Solids **48**, 1107 (2000)
2 K.M. Crosby, R.M. Bradley: Phys. Rev. E **59**, 2542 (1999)
3 K. Leung, Z. Neda: Phys. Rev. Lett. **85**, 662 (2000)
4 Z. Neda, K.T. Leung, L. Jozsa, M. Ravasz: Phys. Rev. Lett. **88**, 095502 (2002)
5 K.T. Leung, L. Jozsa, M. Ravasz, Z. Neda: Nature **410**, 166 (2001)
6 A.T. Skjeltop, P. Meakin: Nature **335**, 424 (1988)
7 A. Yuse, M. Sano: Nature **362**, 329 (1993)
8 T. Bai, D.D. Pollard, H. Gao: Nature **403**, 753 (2000)
9 D. Hull: *Fractography* (Cambridge University Press, Cambridge 1999)
10 B.J. Macnulty: J. Mat. Sci. **6**, 1070 (1971)
11 T.J. Garino: Mat. Res. Soc. Symp. Proc. **180**, 497 (1990)
12 D.A. Dillard, J.A. Hinkley, W.S. Johnson, T.L. Clair: J. Adhesion **44**, 51 (1994)
13 C.J. Brinker, G. Scherer: *Sol-Gel Science* (Academic Press, San Diego, 1990)